

Tensor analyzing powers in ${}^4\text{He}(d,d){}^4\text{He}$ elastic scattering between 17 and 45 MeV

E. J. Stephenson,* H. E. Conzett, R. M. Larimer, B. T. Leemann, R. Roy,[†] and P. von Rossen

Lawrence Berkeley Laboratory, Berkeley, California 94720

(Received 3 August 1979)

Angular distribution measurements were made of the differential cross section $d\sigma/d\Omega$ and the tensor analyzing powers A_{yy} and A_{xx} in d - α elastic scattering between deuteron beam energies of 17 and 45 MeV. The analyzing powers are large over this energy range and suitable for use as a secondary polarization standard. The use of rapid spin flip on the polarized ion source appreciably reduced experimental errors.

[NUCLEAR REACTIONS ${}^4\text{He}(d,d){}^4\text{He}$ elastic scattering, $E_d=17-45$ MeV; measured $d\sigma/d\Omega$, tensor analyzing powers A_{yy} and A_{xx} .]

I. INTRODUCTION

Extensive and precise measurements have been made of the analyzing powers in d - α elastic scattering at tandem energies. The first such experiments¹⁻³ involved double scattering to observe the corresponding polarization moments. Since then, both the vector⁴⁻⁷ and all tensor⁸⁻¹¹ analyzing powers have been measured with polarized deuteron beams. In an effort to completely determine the scattering matrix, an additional 24 polarization transfer coefficients have also been observed.¹² Only the measurements of Ref. 8 are inconsistent with other work, being low by about a factor of two. Recently experiments have begun to extend the energy range of these measurements up to 45 MeV.¹³

The analyzing power measurements have been used primarily in phase shift analyses.^{6, 14-17} With even the earliest efforts,¹⁴ it was clear that analyzing power measurements were needed in addition to cross section data to remove ambiguities in the phase shifts. The energy dependence of the derived phase shifts then confirmed¹⁴ the presence of the 2^+ and 1^+ $T=0$ states in ${}^6\text{Li}$ near 5 MeV. As the extent and precision of measurements improved, they served both as a testing ground for previous analyses, and as input to other sorts of model calculations.¹⁸

Throughout this energy region, the analyzing powers are large and vary smoothly with energy, making d - α elastic scattering attractive as a polarization analyzer. The analyzing power was first calibrated absolutely in a comparison with the ${}^{16}\text{O}(d, \alpha_1){}^{14}\text{N}$ reaction, whose analyzing powers are constrained by the 0^+ spin and parity of the ${}^{14}\text{N}$ final state.^{19, 20} In addition, there are energies and angles where the analyzing power $A_{yy}=1$. This possibility, first noted in Ref. 10, was later confirmed on the basis of a phase shift analysis.²¹ Thus d - α elastic scattering is useful both as a

primary as well as a secondary polarization standard.

For experiments with tensor polarized deuteron beams at energies up to 50 MeV, a polarization standard is clearly needed. Besides having large analyzing powers that vary slowly with energy, the d - α elastic scattering system is an attractive analyzer because of its large cross section and the ease with which the scattered particles can be observed. Complete angular distribution measurements are useful for phase shift analysis, although the increased influence of absorption at higher energies makes the study of more resonances in ${}^6\text{Li}$ seem unlikely.¹⁷ It would also prove fortunate if additional absolute calibration points could be found.

In this paper, we report angular distribution measurements of the tensor analyzing powers A_{yy} and A_{xx} between 17 and 45 MeV, and at center-of-mass angles from 30° to 160° . Angular distributions were measured at 17 MeV to compare with existing measurements,^{10, 11} and the calibration of the polarimeter adjusted to give agreement at this energy. The differential cross section was measured along with the analyzing powers. The energies in this experiment overlap with the disputed measurements of Ref. 8. After the survey of d - α scattering was completed, selected points with extreme values of the tensor analyzing power were remeasured with greater precision using a recently completed rapid spin flip scheme for the polarized ion source. The measurements presented here complement the vector analyzing power angular distributions presented in Ref. 22.

II. EXPERIMENTAL TECHNIQUE

The polarized ion beam was generated in an atomic beam source.²³ The principles of operation are reviewed in Ref. 24. The beam quantization axis is constrained to be parallel to the cyclotron

main field or perpendicular to the beam direction, and the analyzing powers measured are most conveniently expressed in Cartesian tensors.^{25,26} Two tensor analyzing power measurements are possible. One, in which the quantization axis is perpendicular to the scattering plane, yields polarized cross sections²⁶ given by

$$\sigma = \sigma_0 \left(1 + \frac{3}{2} p_y A_y + \frac{1}{2} p_{yy} A_{yy} \right). \quad (1)$$

The other, in which the quantization axis lies in the scattering plane, yields

$$\sigma = \sigma_0 \left(1 + \frac{1}{2} p_{xx} A_{xx} \right). \quad (2)$$

The notation for beam polarization (p) and analyzing power (A) follows the Madison Convention.²⁵ These two cases were measured in separate experiments, between which the scattering chamber was rotated about the beam line.

In normal operation, the intermediate field rf transition on the polarized ion source is used to produce a tensor polarized beam with a vector polarized component of about $\frac{1}{3}$ the magnitude of the tensor component. All of the d - α angular distributions were measured by comparing counting rates with this transition on and off (method I). Later the ion source was modified to allow the weak field and intermediate field rf oscillators to be turned on and off under remote control. Magnetic shielding was added to isolate the two rf regions. When the weak field transition is added, the signs of the tensor and vector beam moments reverse.²⁴ Some d - α measurements were repeated by comparing the counting rates with positive and negative tensor moments and with unpolarized beam (method II). The second method provides greater efficiency in measuring the tensor analyzing powers, and rapid cycling through the three polarization states greatly reduces the systematic errors from slow variations in beam optics and electronic signal processing.

This experiment was conducted with two scattering chambers in series along the beam line. The first, equipped with remotely adjustable detector arms, was used to measure the angular distributions. The beam was recollimated into the second scattering chamber or polarimeter, where deuterium scattering from ${}^4\text{He}$ was used as an analyzer to measure the beam polarization. In both scattering chambers, detectors were placed symmetrically on either side of the beam.

For method I, the tensor polarization of the beam was negative. The polarized and unpolarized beams were run for the same integrated current in a Faraday cup following the polarimeter. The beam on target in the main scattering chamber was measured by two monitor detectors located at 21° to the beam axis. In terms of the beam po-

larizations p_y and p_{yy} , the analyzing powers were calculated from

$$A_{yy} = \frac{1}{p_{yy}} \left[\frac{M_0}{M_-} \left(\frac{C_{-L}}{C_{0L}} + \frac{C_{-R}}{C_{0R}} \right) - 2 \right] \quad (3)$$

and

$$A_y = \frac{M_0}{3p_y M_-} \left(\frac{C_{-L}}{C_{0L}} - \frac{C_{-R}}{C_{0R}} \right). \quad (4)$$

The sum of the counts in the monitor detectors for each run is given by M_- and M_0 . The elastic scattering events recorded in the detectors in either the polarimeter or scattering chamber are given by C , with $-$ and 0 denoting polarization states and L and R denoting sides of the beam. Equations (3) and (4) were used for the beam polarization as well by exchanging p and A and setting $M_0/M_- = 1$. The analyzing power at the monitor detector position was measured in a separate run with a Faraday cup immediately after the scattering chamber to normalize the beam current. Because the collimators preceding the polarimeter accepted only about 20% of the beam, the polarization was usually determined with less precision than could be obtained for the analyzing powers in the main scattering chamber. So the polarizations for successive runs were fit to a straight line, and the straight line value for a given run used for the beam polarization in that run. Beam polarizations for the runs to measure monitor detector analyzing power were taken from the straight line value. Individual beam polarization measurements were consistent within the statistical errors with the straight line fit; and the magnitude of the beam polarization varied by only a few percent during the course of running at one beam energy. Angular distributions computed with beam polarizations from the linear fit were generally smoother than distributions computed using individual polarization measurements.

Experiments conducted with method II proceeded in a similar fashion, except that a positively polarized tensor beam was added, and the rapid spin flip eliminated the need for monitor detectors in the main scattering chamber. The polarization state of the beam was changed every time a predetermined amount of charge was collected in the polarimeter Faraday cup, usually about once a second. The possibility exists that the magnitude of the polarization was not the same in the two polarized states, so it is useful to define quantities for the average and difference:

$$p_{yy} = \frac{1}{2} (p_{yy}^{(+)} - p_{yy}^{(-)}), \quad (5)$$

$$\Delta p_{yy} = \frac{1}{2} (p_{yy}^{(+)} + p_{yy}^{(-)}),$$

where $p_{yy}^{(\pm)}$ refer to the positive and negative beam moments. Similar quantities can be defined for

the vector beam moment. In terms of the polarimeter analyzing powers and the number of events recorded, the beam moments become

$$\begin{aligned}
 p_{yy} &= \frac{1}{2A_{yy}} (Q_L^- + Q_R^-), \\
 \Delta p_{yy} &= \frac{1}{2A_{yy}} (Q_L^+ + Q_R^+ - 4), \\
 p_y &= \frac{1}{6A_y} (Q_L^- - Q_R^-), \\
 \Delta p_y &= \frac{1}{6A_y} (Q_L^+ - Q_R^+),
 \end{aligned} \tag{6}$$

where

$$\begin{aligned}
 Q_L^\pm &= \frac{C_{+L} \pm C_{-L}}{C_{0L}}, \\
 Q_R^\pm &= \frac{C_{+R} \pm C_{-R}}{C_{0R}}.
 \end{aligned}$$

The number of events C per detector per spin direction is defined similarly to method I. Using these moments (or a linear fit to them), the analyzing powers measured in the main scattering chamber are given by

$$A_{yy} = \frac{-2}{D} [R_L R_R p_y^{(-)} + p_y^{(+)} - (R_L + R_R) \Delta p_y], \tag{7}$$

$$A_y = \frac{2}{3D} (R_L - R_R) p_{yy}, \tag{8}$$

where

$$\begin{aligned}
 R_L &= C_{+L}/C_{-L}, \\
 R_R &= C_{+R}/C_{-R}, \\
 D &= R_L R_R p_{yy}^{(-)} p_y^{(-)} + p_{yy}^{(+)} p_y^{(+)} \\
 &\quad - (R_L + R_R) (\Delta p_{yy} \Delta p_y - p_{yy} p_y),
 \end{aligned}$$

The measurement of the tensor analyzing power A_{xx} uses the same formulas [Eqs. (3) and (7)] as A_{yy} . Since the polarimeter does not rotate about the beam axis with the scattering chamber, the p_{yy} moment measured in the polarimeter is assumed to be the same as the p_{xx} moment in the scattering chamber. The tilt of the main chamber scattering plane is known to within $\frac{1}{4}^\circ$. Values of A_x obtained from Eqs. (4) and (8) should be zero if parity is conserved, and serve as a useful check on the internal consistency of the measurements.

Relative errors in the measured analyzing powers were computed by propagating the errors in the initial quantities through the method I and II formulas. For each angular distribution, the analyzing power of the polarimeter acts as a scale factor, and that error was taken to be zero. Relatively little background was subtracted from the particle spectra, so the error in the count rate

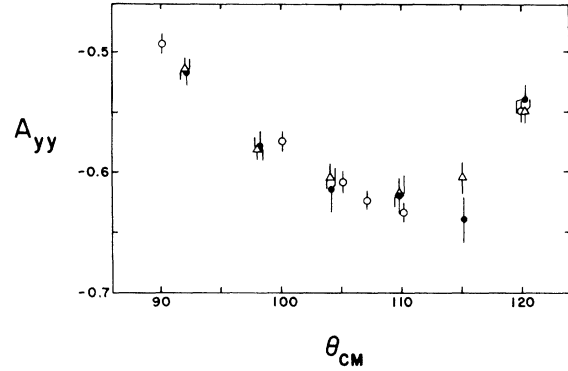


FIG. 1. Comparison of A_{yy} measurements at 17 MeV between $\theta_{c.m.} = 90^\circ$ and 120° from this work (solid points), Ref. 10 (open triangles), and Ref. 11 (open circles). The calibration of the tensor polarimeter was adjusted to give the best agreement with the measurements of Ref. 10.

was assumed to be equal to the square root of the number of counts. The integrators of beam current were checked and found to have an error of about 0.25%, which was included in the analysis of beam polarization. The error in the beam polarization was taken to be the rms deviation of the individual measurements about the line divided by the square root of the number of measurements. The error in the absolute calibration will be discussed later.

The calibration of the polarimeter was adjusted so that the A_{yy} angular distribution measured at 17 MeV matched the results of Ohlsen *et al.*¹⁰ in the range $\theta_{c.m.} = 90^\circ - 120^\circ$, as shown in Fig. 1. Ohlsen's measurements were normalized by the quench ratio method,²⁷ and are accurate to about 2%. New measurements by Brown *et al.*¹¹ do not substantially change the value of the calibration. The calibrated polarimeter was used at higher beam energies by degrading the beam energy between the two scattering chambers in an aluminum absorber. To minimize beam losses from multiple scattering ahead of the polarimeter, new calibration points were established at 25 and 35

TABLE I. Average beam energies in scattering chamber and polarimeter and polarimeter laboratory scattering angle.

E_{scat}	E_{pol}	θ_{pol}
17.0	16.5	80°
19.7	16.7	80°
24.9	16.8	80°
29.9	24.9	85°
35.0	25.0	85°
40.1	35.1	85°
45.2	35.1	85°

TABLE II. Nominal slit geometry in scattering chamber and polarimeter.

Location	Observed particle	Angular range	Front width (cm)	Back width (cm)	Back height (cm)	R^a (cm)	h^b (cm)
Scattering chamber	α	$10^\circ\text{--}35^\circ$	0.25	0.25	0.4	26.9	15.4
Scattering chamber	d	$20^\circ\text{--}70^\circ$	0.35	0.35	0.4	26.9	15.4
Scattering chamber	d	$60^\circ\text{--}90^\circ$	0.4	0.4	0.4	26.9	15.4
Polarimeter	d	$80^\circ\text{--}85^\circ$	0.4	0.4	0.4	15.9	8.9

^a R is gas cell to back slit distance.

^b h is front to back slit distance.

MeV based on measurements with the polarimeter operating at lower energy. The average energy of the beam in the scattering chamber and polarimeter for each angular distribution is given in Table I. The beam energy of the cyclotron is known from magnetic analysis²⁸ to better than $\frac{1}{2}\%$.

Differential cross sections were computed from the counting rates measured with an unpolarized beam. The geometry of the gas cell was included by using Eq. (22) of Ref. 29. An absolute normalization of the beam current was obtained when the Faraday cup was placed between the scattering chamber and the polarimeter to calibrate the mon-

itor detectors. The results from all detectors at the same angle were averaged.

The incident and scattered beams were collimated using tantalum slits. The beam at the entrance to the scattering chamber was collimated to 0.3 cm wide and 0.6 cm high about 40 cm ahead of the 7.6 cm diameter gas cell. The beam was recollimated after the aluminum absorber at the entrance to the polarimeter by a 1 cm diameter circular aperture. The scattering chamber and polarimeter slits were rectangular, with dimensions given in Table II. The polarimeter scattering angle as a function of energy is given in Table I. Geometric corrections to A_{yy} following the argu-

TABLE III. Cross sections and tensor analyzing powers $E_d=17.0$ MeV.

$\theta_{c.m.}$	$d\sigma/d\Omega$ (mb/sr)	A_{yy}	A_{xx}
30.0	170	0.055 ± 0.010	-0.062 ± 0.016
33.7	113	0.102 ± 0.009	-0.072 ± 0.016
37.3	70.7	0.124 ± 0.010	-0.109 ± 0.015
41.0	42.9	0.160 ± 0.011	-0.146 ± 0.016
44.7	26.0		-0.130 ± 0.017
48.3	16.5	0.220 ± 0.014	-0.112 ± 0.018
51.9	12.3	0.188 ± 0.014	-0.011 ± 0.019
55.4	12.0	0.133 ± 0.015	0.062 ± 0.018
59.0	13.4	0.057 ± 0.010	0.079 ± 0.011
65.9	19.0	-0.144 ± 0.014	0.127 ± 0.013
72.8	25.6	-0.224 ± 0.014	0.174 ± 0.016
79.5	31.3	-0.329 ± 0.015	0.210 ± 0.016
86.0	35.8	-0.423 ± 0.010	0.292 ± 0.009
92.2	38.8	-0.527 ± 0.011	0.348 ± 0.010
98.3	39.7	-0.579 ± 0.012	0.380 ± 0.012
104.2	37.2	-0.615 ± 0.017	0.371 ± 0.016
109.8	33.6	-0.619 ± 0.015	0.363 ± 0.017
115.2	28.6	-0.641 ± 0.019	0.361 ± 0.018
120.2	23.8	-0.540 ± 0.012	0.288 ± 0.012
125.0	19.4	-0.450 ± 0.015	0.152 ± 0.015
130.0	16.0	-0.192 ± 0.013	-0.049 ± 0.017
135.0	14.5	0.131 ± 0.012	-0.288 ± 0.019
140.0	15.0		-0.428 ± 0.021
145.0	16.9	0.438 ± 0.013	-0.470 ± 0.021
150.0	20.5	0.393 ± 0.011	-0.374 ± 0.019
155.0	25.3	0.286 ± 0.010	-0.264 ± 0.018
160.0	30.2	0.161 ± 0.011	-0.170 ± 0.018

TABLE IV. Cross sections and tensor analyzing powers $E_d=19.7$ MeV.

$\theta_{c.m.}$	$d\sigma/d\Omega$ (mb/sr)	A_{yy}	A_{xx}
30.0	177	0.051 ± 0.025	-0.062 ± 0.019
33.7	120	0.092 ± 0.022	-0.128 ± 0.018
37.4	66.6	0.109 ± 0.022	-0.071 ± 0.016
41.0	40.2	0.103 ± 0.024	-0.127 ± 0.017
44.7	24.9	0.102 ± 0.021	-0.113 ± 0.018
48.3	19.1	0.069 ± 0.025	-0.133 ± 0.019
51.9	17.0	-0.040 ± 0.027	0.041 ± 0.019
55.4	18.1	-0.041 ± 0.027	0.093 ± 0.018
59.0	19.8	-0.132 ± 0.019	0.116 ± 0.013
66.0	24.0	-0.138 ± 0.027	0.126 ± 0.018
72.8	26.7	-0.118 ± 0.027	0.154 ± 0.018
79.5	28.5	-0.259 ± 0.029	0.209 ± 0.018
86.0	30.2	-0.390 ± 0.022	0.281 ± 0.012
92.3	30.3	-0.462 ± 0.024	0.328 ± 0.012
98.4	32.4	-0.524 ± 0.032	0.396 ± 0.013
104.2	30.5	-0.547 ± 0.012	0.420 ± 0.018
109.8	27.5	-0.607 ± 0.034	0.388 ± 0.018
115.2	23.9	-0.576 ± 0.015	0.325 ± 0.019
120.2	19.3	-0.525 ± 0.032	0.268 ± 0.013
125.0	15.7	-0.380 ± 0.030	0.115 ± 0.017
130.0	12.8	-0.121 ± 0.027	-0.110 ± 0.020
135.0	11.6	0.208 ± 0.024	-0.324 ± 0.022
140.0	11.1	0.437 ± 0.021	-0.409 ± 0.024
145.0	12.8	0.518 ± 0.024	-0.464 ± 0.023
150.0	14.9	0.470 ± 0.023	-0.406 ± 0.021
155.0	20.2	0.357 ± 0.022	-0.248 ± 0.021
160.0	22.1	0.228 ± 0.025	-0.128 ± 0.021

TABLE V. Cross sections and tensor analyzing powers $E_d=24.9$ MeV. Points marked with an asterisk were taken with method II.

$\theta_{c.m.}$	$d\sigma/d\Omega$ (mb/sr)	A_{yy}	A_{xx}
30.0	171	0.108 ± 0.018	-0.114 ± 0.022
33.7	106	0.156 ± 0.018	-0.159 ± 0.023
37.4	63.3		-0.168 ± 0.023
41.0	39.5	0.074 ± 0.018	-0.160 ± 0.024
44.7	28.2	0.016 ± 0.019	-0.103 ± 0.012
48.3	25.0	-0.147 ± 0.020	0.031 ± 0.023
51.9	25.8	-0.214 ± 0.021	0.105 ± 0.023
55.5	27.9	-0.245 ± 0.022	0.145 ± 0.023
59.0	29.9	-0.212 ± 0.021	0.137 ± 0.022
62.5	30.5	-0.208 ± 0.021	
66.0	30.1	-0.164 ± 0.015	
72.8	26.2	-0.131 ± 0.021	
79.5	22.4	-0.140 ± 0.023	
86.0	20.5	-0.215 ± 0.020	
92.3	20.0	-0.325 ± 0.018	
94.9			$0.354 \pm 0.009^*$
98.4	20.0	-0.447 ± 0.027	
99.9		$-0.477 \pm 0.008^*$	$0.386 \pm 0.008^*$
104.2	19.0	-0.571 ± 0.029	
104.9		$-0.562 \pm 0.008^*$	$0.388 \pm 0.008^*$
109.9	17.5	$-0.619 \pm 0.008^*$	$0.392 \pm 0.008^*$
115.1	15.2	$-0.631 \pm 0.008^*$	
119.9	12.7	$-0.583 \pm 0.008^*$	0.257 ± 0.023
124.9	10.5	-0.398 ± 0.026	0.127 ± 0.023
129.9	8.83	-0.068 ± 0.022	-0.120 ± 0.027
134.9	8.14	0.310 ± 0.020	$-0.337 \pm 0.009^*$
140.0	8.26	$0.605 \pm 0.008^*$	$-0.511 \pm 0.008^*$
145.0	8.94	$0.744 \pm 0.008^*$	$-0.512 \pm 0.008^*$
150.0	9.94	$0.753 \pm 0.009^*$	$-0.449 \pm 0.008^*$
155.0	11.0	$0.652 \pm 0.009^*$	-0.275 ± 0.027
160.0	12.3	$0.537 \pm 0.008^*$	-0.129 ± 0.023

ments of Ref. 29 were made for the polarimeter, and amounted to 0.2% of A_{yy} at 17 MeV, 0.5% at 25 MeV, and 2.2% at 35 MeV. The corrections were expected to be smaller for the scattering chamber measurements and were neglected.

Scattered particles were detected in silicon detectors telescopes. The signals from the front and back detectors were separated by particle type in an analog particle identification circuit.³⁰ Pulse height spectra of deuteron or α -particle events were stored in an on-line computer for later analysis. A pulser creating deuteron or α -particle-like events at higher energy was used to measure the dead time. Background was subtracted from the pulse height spectra when appropriate.

III. RESULTS

The average value of the beam polarization was relatively constant for one beam energy, but varied with changing beam energy over the range $p_{yy} = 0.74-0.94$. These values did not reproduce when energy settings were repeated. The errors, com-

TABLE VI. Cross sections and tensor analyzing powers $E_d=29.9$ MeV.

$\theta_{c.m.}$	$d\sigma/d\Omega$ (mb/sr)	A_{yy}	A_{xx}
30.0	168	0.144 ± 0.016	-0.157 ± 0.013
33.7	100	0.166 ± 0.015	-0.177 ± 0.014
37.4	58.6	0.178 ± 0.014	-0.222 ± 0.014
41.1	37.1	0.120 ± 0.015	-0.152 ± 0.014
44.7	29.6	-0.036 ± 0.017	-0.063 ± 0.014
48.3	29.5	-0.178 ± 0.017	0.063 ± 0.014
51.9	32.5	-0.258 ± 0.018	0.131 ± 0.013
55.5	35.2	-0.256 ± 0.018	0.119 ± 0.013
59.0	36.4	-0.244 ± 0.018	0.132 ± 0.012
62.6	35.6	-0.235 ± 0.018	0.132 ± 0.012
66.0	32.9	-0.195 ± 0.012	0.113 ± 0.008
72.9	25.0	-0.133 ± 0.018	0.098 ± 0.012
79.5	17.6	-0.129 ± 0.019	0.162 ± 0.013
86.0	13.7	-0.102 ± 0.017	0.312 ± 0.015
92.3	11.9	-0.250 ± 0.016	0.398 ± 0.010
98.4	11.7	-0.381 ± 0.023	0.447 ± 0.014
104.3	11.4	-0.502 ± 0.025	0.430 ± 0.014
109.9	10.8	-0.621 ± 0.018	0.421 ± 0.010
115.1	9.46	-0.715 ± 0.020	0.362 ± 0.011
120.2	8.05	-0.656 ± 0.026	0.298 ± 0.011
124.9	7.00	-0.421 ± 0.023	0.135 ± 0.018
129.9	6.38	-0.050 ± 0.018	-0.049 ± 0.019
134.9	6.22	0.374 ± 0.012	-0.252 ± 0.020
139.9	6.51	0.685 ± 0.020	-0.394 ± 0.020
145.0	6.90	0.872 ± 0.021	-0.390 ± 0.019
150.0	7.34	0.901 ± 0.021	-0.391 ± 0.018
155.0	7.41	0.828 ± 0.021	-0.263 ± 0.017
160.0	7.32	0.722 ± 0.020	-0.137 ± 0.016

puted from the deviation of the points from a linear fit, varied from 0.008 to 0.037 for method I and from 0.006 to 0.009 for method II. The improvement with method II result from the factor of two increase in the cross section change observed in a run, and the elimination of errors from slow systematic changes by rapid spin flip.

If the rf transitions worked perfectly,²⁴ then the beam moments defined in Eq. (5) would satisfy $p_{yy}/p_y = R=3$ and $\Delta p_{yy} = \Delta p_y = 0$. The polarizations obtained in method II differed substantially from this prediction. The ratio R varied from 2.49 to 2.79 and Δp_y varied from 0.042 to 0.052. This behavior can be understood if the intermediate field transition is incomplete. The tensor polarization p_{yy} in Eq. (5) is reduced, p_y remains the same, and Δp_y increases, so that

$$R = p_{yy}/p_y = 3(1 - 3\Delta p_y). \quad (9)$$

This formula is consistent with the measurements. For the spin state with the intermediate field rf transition operating alone, $R=3$. The nonzero value of Δp_y makes a significant contribution to the final values of A_{yy} and A_y calculated from Eqs. (7) and (8), and its measurement with an unpolarized beam was essential.

TABLE VII. Cross sections and tensor analyzing powers $E_d=35.0$ MeV. Points marked with an asterisk were taken with method II.

$\theta_{c.m.}$	$d\sigma/d\Omega$ (mb/sr)	A_{yy}	A_{xx}
30.0	166	0.142 ± 0.014	-0.106 ± 0.033
33.7	92.6	0.192 ± 0.013	-0.224 ± 0.023
37.4	53.2	0.216 ± 0.013	-0.260 ± 0.027
41.1	34.1	0.157 ± 0.014	-0.218 ± 0.023
44.7	28.4	-0.021 ± 0.015	-0.075 ± 0.020
48.4	29.8	-0.123 ± 0.016	0.043 ± 0.020
52.0	33.5	-0.198 ± 0.016	0.149 ± 0.018
55.5	36.5	-0.225 ± 0.016	0.168 ± 0.018
59.1	37.3	-0.226 ± 0.016	0.137 ± 0.018
62.6	35.9	-0.211 ± 0.015	0.148 ± 0.018
66.1	32.5	-0.206 ± 0.011	0.095 ± 0.019
72.9	22.9	-0.134 ± 0.016	0.107 ± 0.018
79.6	14.4	-0.081 ± 0.017	0.170 ± 0.019
86.1	9.39	0.004 ± 0.017	0.296 ± 0.020
92.4	7.63	-0.006 ± 0.013	0.450 ± 0.014
94.9			0.476 ± 0.015*
98.5	7.26	-0.182 ± 0.020	0.512 ± 0.015
99.9		-0.192 ± 0.010*	0.498 ± 0.016*
104.3	7.09	-0.303 ± 0.022	0.471 ± 0.021
104.9		-0.332 ± 0.007*	0.469 ± 0.021*
109.9	6.38	-0.486 ± 0.007*	0.345 ± 0.015*
115.1	5.41	-0.594 ± 0.007*	0.278 ± 0.013
120.2	4.58	-0.542 ± 0.011*	0.151 ± 0.016
124.9	4.12	-0.345 ± 0.023	0.059 ± 0.023
129.9	4.08	0.075 ± 0.019	-0.147 ± 0.024
134.9	4.48	0.501 ± 0.017	-0.284 ± 0.026*
139.9	5.14	0.753 ± 0.006*	-0.331 ± 0.026*
144.9	5.55	0.883 ± 0.006*	-0.393 ± 0.027*
150.0	5.47	0.937 ± 0.006*	-0.333 ± 0.026*
155.0	5.23	0.904 ± 0.006*	-0.325 ± 0.027
160.0	4.77	0.852 ± 0.012*	-0.063 ± 0.035

Final angular distributions of differential cross section and the analyzing powers A_{yy} and A_{xx} are presented in Tables III–IX and Figs. 2–4. Points marked with an asterisk were taken with method II. Where more than one measurement existed at a given angle, the results were averaged. In the case of the analyzing powers, the average was weighted by the reciprocal of the square of the error. With method I, the ratio of the monitor detector counts in the polarized and unpolarized runs varied by a few percent from run to run. These fluctuations represented real changes in the beam current on target, since the analyzing power angular distributions were noticeably less smooth when monitor corrections were not made. With the rapid spin flip of method II, these ratios were constant from run to run within the statistical error. Occasional analyzing power points were discarded if some consistency condition, such as the monitor ratio or the value of A_x , fell many standard deviations outside its normal range.

The analyzing power errors given in Tables

TABLE VIII. Cross sections and tensor analyzing powers $E_d=40.1$ MeV.

$\theta_{c.m.}$	$d\sigma/d\Omega$ (mb/sr)	A_{yy}	A_{xx}
30.0	157	0.115 ± 0.013	-0.160 ± 0.017
33.7	90.8	0.145 ± 0.013	-0.157 ± 0.015
37.4	50.1	0.183 ± 0.013	-0.211 ± 0.016
41.1	32.1	0.132 ± 0.013	-0.209 ± 0.016
44.8	26.2	-0.008 ± 0.014	-0.075 ± 0.012
48.4	27.7	-0.122 ± 0.014	0.080 ± 0.013
52.0	30.5	-0.195 ± 0.015	0.068 ± 0.012
55.6	32.6	-0.195 ± 0.015	0.102 ± 0.011
59.1	32.5	-0.210 ± 0.015	0.071 ± 0.010
62.6	30.5	-0.212 ± 0.016	0.090 ± 0.010
66.1	27.1	-0.189 ± 0.011	0.081 ± 0.016
72.9	18.2	-0.149 ± 0.015	0.091 ± 0.010
79.6	10.7	-0.067 ± 0.015	0.179 ± 0.011
86.1	6.34	0.121 ± 0.016	0.280 ± 0.016
92.4	4.79	0.233 ± 0.012	0.487 ± 0.010
98.5	4.41	0.130 ± 0.018	0.541 ± 0.013
104.4	4.24	-0.060 ± 0.018	0.468 ± 0.014
110.0	3.78	-0.321 ± 0.015	0.310 ± 0.022
115.1	3.07	-0.547 ± 0.019	0.169 ± 0.012
119.9	2.64	-0.586 ± 0.027	0.024 ± 0.017
124.9	2.55	-0.354 ± 0.023	-0.093 ± 0.019
129.9	2.86	0.058 ± 0.017	
134.9	3.44	0.420 ± 0.020	-0.217 ± 0.019
139.9	3.95	0.672 ± 0.021	-0.313 ± 0.020
144.9	4.19	0.761 ± 0.022	-0.366 ± 0.021
149.9	4.04	0.843 ± 0.024	-0.277 ± 0.020
155.0	3.63	0.813 ± 0.023	-0.157 ± 0.019
160.0	3.12	0.721 ± 0.021	-0.053 ± 0.020

III–IX are statistical. They contain contributions from the polarimeter and monitor detectors as well as the number of events detected, and are reasonable estimates of the relative error in each angular distribution. The absolute error is more difficult to determine, in part because of uncertainties in matching the measurements of Refs. 10 and 11 to our results. Originally, our results (shown by the solid dots in Fig. 1) were scaled to agree best to A_{yy} from Ref. 10 (open triangles) between $\theta_{c.m.} = 90^\circ$ and 120° , excluding our point at 115° . The work of Ref. 11 (open circles) was completed later and has somewhat better statistics. It does not suggest any significant scale shift in this angular range, even though the trend of the measurements is somewhat different. The calibration error is given as 2% (0.012 at 110°) in Ref. 10 and 1.5% (0.009) in Ref. 11. The calibration error increases as the polarimeter is stepped up in energy. For measurements above 17 MeV we add 1.3% for statistics and 0.3% for systematic errors. The systematic errors include estimates for the effect of errors in the beam energy, aluminum degrader energy loss, geometric corrections in the polarimeter, and the setting of the detector arm angles. The thick-

TABLE IX. Cross sections and tensor analyzing powers $E_d = 45.2$ MeV. Points marked with an asterisk were taken with method II.

$\theta_{c.m.}$	$d\sigma/d\Omega$ (mb/sr)	A_{yy}	A_{xx}
30.1	138	0.118 ± 0.019	-0.110 ± 0.009
33.8	78.1	0.161 ± 0.013	-0.138 ± 0.010
37.5	43.4	0.165 ± 0.013	-0.176 ± 0.012
41.1	28.2	0.115 ± 0.013	-0.146 ± 0.011
44.8	23.9	0.009 ± 0.014	-0.048 ± 0.007
48.4	24.2	-0.088 ± 0.015	0.036 ± 0.006
52.0	26.0	-0.133 ± 0.016	0.074 ± 0.007
55.6	26.9	-0.153 ± 0.015	0.101 ± 0.007
59.1	26.1	-0.178 ± 0.016	0.111 ± 0.015
62.6	23.9	-0.183 ± 0.016	0.120 ± 0.008
66.1	20.4	-0.205 ± 0.016	0.095 ± 0.008
73.0			0.080 ± 0.009
79.6	7.08	-0.053 ± 0.013	0.135 ± 0.012
86.1	4.03	0.233 ± 0.017	0.285 ± 0.014
92.4	2.97	0.444 ± 0.020	0.506 ± 0.028
98.5		0.404 ± 0.021	0.500 ± 0.029
104.4	2.72	0.218 ± 0.017	0.368 ± 0.023
104.9		$0.171 \pm 0.016^*$	
110.0	2.34	$-0.077 \pm 0.013^*$	0.201 ± 0.014
114.9	1.95	$-0.357 \pm 0.016^*$	0.093 ± 0.013
119.9	1.68	$-0.507 \pm 0.015^*$	0.028 ± 0.021
124.9	1.69	$-0.373 \pm 0.013^*$	-0.034 ± 0.012
129.9	2.08	0.041 ± 0.020	-0.123 ± 0.013
134.9	2.57	0.331 ± 0.018	-0.182 ± 0.014
139.9	3.06	0.543 ± 0.019	-0.238 ± 0.016
144.9	3.14	$0.702 \pm 0.015^*$	-0.297 ± 0.019
149.9	2.93	$0.779 \pm 0.020^*$	-0.253 ± 0.018
154.9	2.53	$0.784 \pm 0.028^*$	-0.083 ± 0.012
160.0	2.32	$0.628 \pm 0.033^*$	0.126 ± 0.013

ness of the aluminum degraders varied between 69 and 489 mg/cm², and was determined by weighing. Deuteron energy loss was calculated from the tables of Ref. 31, and was assumed to be known to 2%, including absorber thickness errors. Above 25 MeV we add 1.2% for statistics and 1.2% for systematic errors. The increased systematic errors arise from the effect of a steeper dependence in the A_{yy} analyzing power on the uncertainties in the beam energy in the first and second scattering chambers. Above 35 MeV we again add 1.2% for statistics and 1.2% for systematic errors. Assuming an original calibration error of 2% (in part to cover uncertainties in matching 17 MeV angular distributions), the scale error in our analyzing power measurements rises to 2.4% above 17 MeV, 2.9% above 25 MeV, and 3.4% above 35 MeV.

For the differential cross section, the systematic errors were usually greater than the statistical errors. These errors contained contributions from detector arm angle settings, beam steering, particle identification windows, and spectral peak summing methods. Since there were usually at least four measurements (from both A_{yy} and A_{xx}

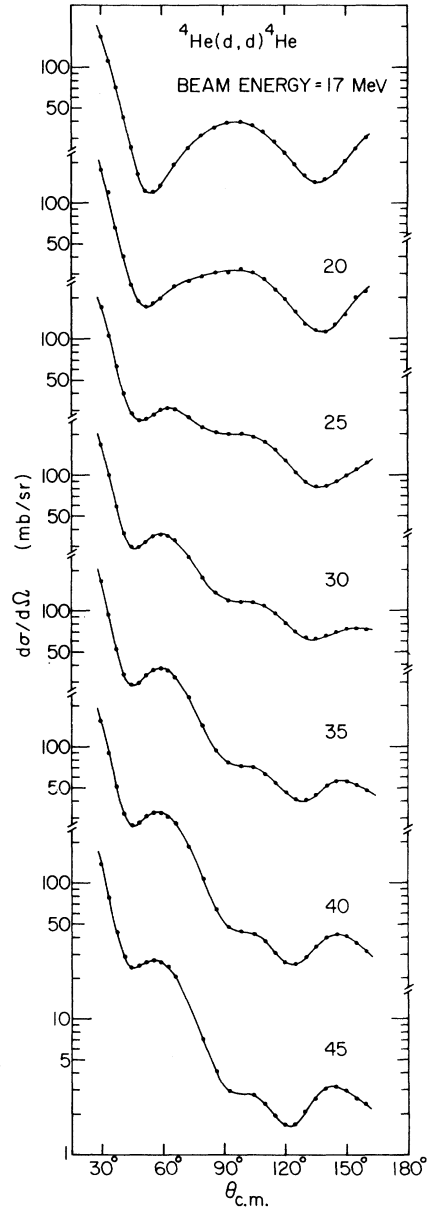


FIG. 2. Differential cross section angular distributions at various beam energies. The curves are a guide to the eye.

angular distributions) at each arm angle, the scatter in the measured values was examined, and found to be less than 2% in almost all cases. Since the scatter varied considerably from point to point, no relative error is included in Tables III-IX. The absolute normalization has additional uncertainties from event counting techniques (3%), monitor detector calibration (2%), gas cell pressure (2%), and geometric corrections (1%), and is probably less than 5%.

The differential cross section was normalized

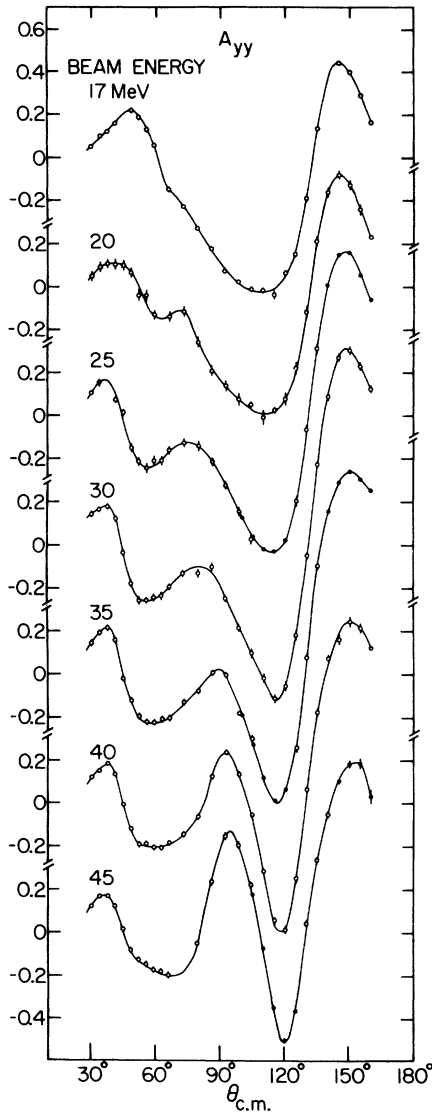


FIG. 3. A_{yy} angular distributions at various beam energies. The open (closed) points were measured with method I (II) (see text for details). The curves are a guide to the eye.

absolutely by comparing the count rate directly to the beam current. Our measurements agree to within 10% with other measurements at these energies.³²⁻³⁶ There is no systematic trend in the discrepancies. In some cases, the quality of agreement varies with angle.

The full A_{yy} and A_{xx} angular distributions may be compared with existing measurements only at 17 MeV. Figure 5 shows the difference between the smooth curves of Figs.3 and 4 and the measurements of Refs. 10 and 11 (lines C and B, respectively). This difference is negative if the measurements fall below the curve. The results of

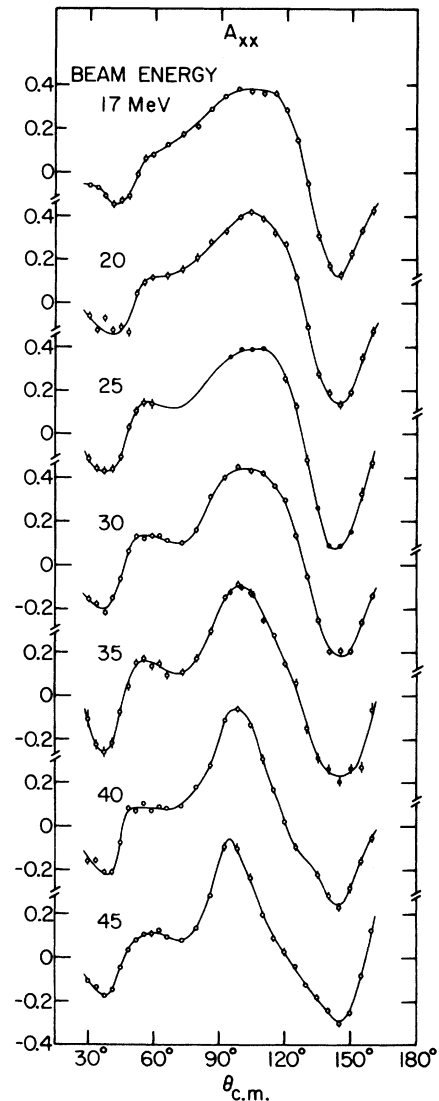


FIG. 4. A_{xx} angular distributions at various beam energies. The open (closed) points were measured with method I (II). The curves are a guide to the eye.

this experiment are included on line A for comparison. In general, our tensor analyzing power results agree with those of Ref. 10 near $\theta_{c.m.} = 110^\circ$ for both A_{yy} and A_{xx} . The more recent re-measurement of Ref. 11 reduced the discrepancies between the two data sets, especially for forward and backward angle measurements of A_{xx} ; but the forward and backward A_{xx} values are still more negative in Ref. 11 than in our results. A few points disagree more than statistics would indicate, suggesting that there are systematic errors beyond those quoted in either reference or this paper. At 20 MeV our measurements follow the trend of Ref. 8, but are about a factor of

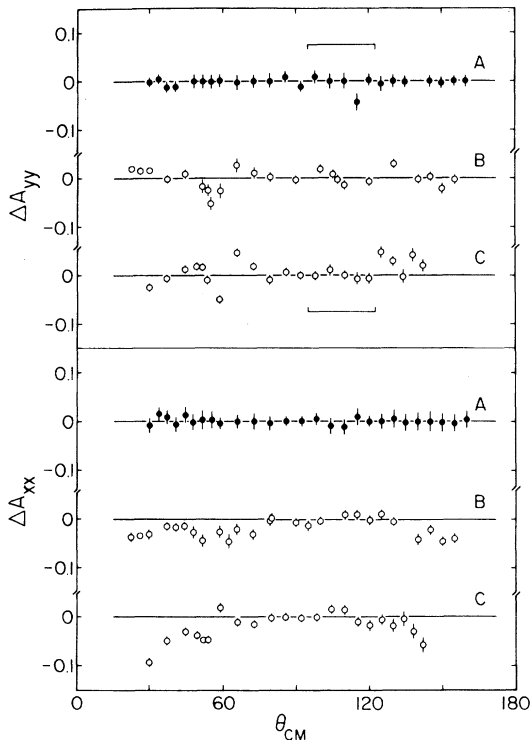


FIG. 5. The difference, ΔA_{yy} and ΔA_{xx} , between the smooth curves of Figs. 3 and 4 and the measurements of this work (A), Ref. 11 (B), and Ref. 10 (C). The bracket for ΔA_{yy} marks the calibration region. All measurements were made at 17 MeV deuteron energy.

two larger in magnitude, as was pointed out for 17 MeV in Ref. 10. Measurements of A_y made simultaneously with A_{yy} agree well with those of Ref. 22. The calibration at 17 MeV was successfully compared to similar measurements¹⁰ at 14 MeV, and to the $A_{yy} = 1$ point²¹ near 21 MeV and 37°. Because of the small cross section near 12 MeV, the statistical precision of the comparison to the absolute calibration point was limited to 7%, much less precise than the calibration values used at 17 MeV.

The tensor analyzing powers are large throughout the energy region from 17 to 45 MeV, especially near 35 MeV where A_{yy} approaches 1. If this back angle maximum in A_{yy} is observed by detecting the recoil α particles, then the beam polarization can be measured with greater efficiency for the same geometry as compared to observing the deuterons elastically scattered near $\theta_{c.m.} = 110^\circ$.

In Ref. 37, it was pointed out that near $E_d = 28.6$ MeV, and $\theta_{c.m.} = 155^\circ$, a possible value of $A_{yy} = 1$ exists. If this is true, then $A_{yy} = 1$ also.³⁸ Since the

measurements of A_{yy} presented here vary smoothly with energy and differ substantially from 1 at 25 and 30 MeV, the possibility of an $A_y = 1$ point is ruled out. Nevertheless, the values of A_y are close to 1, and may provide a useful calibration point for vector polarized beams. Using the measured values of A_{yy} , a limit may be set on A_y based on the rule³⁸:

$$\text{If } A_{yy} = 1 - 3\eta, \text{ then } A_y \leq 1 - \eta.$$

With an interpolated value of $A_{yy} = 0.79$ ($E_d = 28.6$ MeV, $\theta_{c.m.} = 155^\circ$), $A_y \leq 0.93$. A similar result has been reported elsewhere.³⁹ Subsequent to the publication of Ref. 36, the calibration was repeated, and the maximum value of A_y was reduced. The new values²² are consistent with the limits given here.

IV. CONCLUSIONS

In this paper, we reported angular distribution measurements of the differential cross section and tensor analyzing powers A_{yy} and A_{xx} in $d-\alpha$ elastic scattering from 17 to 45 MeV. Along with the vector analyzing power measurements, these results should prove useful in extending earlier phase shift calculations to higher energy. The rapid spin flip sequence used in method II proved to be a significant improvement over method I in both efficiency and precision. This method also revealed a departure from the $\frac{1}{2}$ value of p_y/p_{yy} , indicating that the intermediate field rf transition on the polarized ion source is only 80–90% efficient.

The tensor analyzing powers were found to be large at all energies, with A_{yy} values at 35 MeV approaching unity. Thus $d-\alpha$ elastic scattering can serve as an analyzer for tensor polarized deuterons throughout this energy range. Because of the large backward angle values of A_{yy} , a polarimeter based upon detecting recoil α particles should be strongly considered at higher energies. There are significant contributions to the absolute uncertainty of the tensor analyzing powers from the original calibration and the scattering chamber and polarimeter deuteron energies as well as counting statistics. It is doubtful that large improvements can be made in the precision of the measurements without better calibration values and a more detailed knowledge of the experimental conditions.

This work was performed under the auspices of the U. S. Department of Energy.

- *Present address: Indiana University Cyclotron Facility, Milo B. Sampson Lane, Bloomington, Ind. 47401.
- †Present address: Dept. de Physique, Université Laval, Cité Universitaire, P. Q. Quebec, Canada G1K7P4.
- ¹F. Seiler, S. E. Darden, L. C. McIntyre, and W. G. Weitkamp, Nucl. Phys. 53, 65 (1964); L. G. McIntyre and W. Haerberli, *ibid.* A91, 369 (1967).
 - ²P. G. Young, G. G. Ohlsen, and M. Ivanovich, Nucl. Phys. A90, 41 (1967).
 - ³E. M. Bernstein, G. G. Ohlsen, V. S. Starkovich, and W. G. Simon, Phys. Rev. Lett. 18, 966 (1967); G. G. Ohlsen, V. S. Starkovich, W. G. Simon, and E. M. Bernstein, Phys. Lett. 28B, 404 (1969).
 - ⁴A. Trier and W. Haerberli, Phys. Rev. Lett. 18, 915 (1967).
 - ⁵W. Grüebler, V. König, P. A. Schmelzbach, and P. Marmier, Nucl. Phys. A134, 686 (1969).
 - ⁶L. G. Keller and W. Haerberli, Nucl. Phys. A156, 465 (1970).
 - ⁷C. C. Chang, H. F. Glavish, R. Avida, and R. N. Boyd, Nucl. Phys. A212, 189 (1973).
 - ⁸J. Arvieux, P. Darriulat, D. Garreta, A. Papineau, A. Tarrats, and J. Testoni, Nucl. Phys. A94, 663 (1967).
 - ⁹V. König, W. Grüebler, P. A. Schmelzbach, and P. Marmier, Nucl. Phys. A148, 380 (1970); W. Grüebler, V. König, P. A. Schmelzbach, and P. Marmier, *ibid.* A148, 391 (1970).
 - ¹⁰G. G. Ohlsen, P. A. Lovoi, G. C. Salzman, U. Meyer-Berkhout, C. K. Mitchell, and W. Grüebler, Phys. Rev. C 8, 1262 (1973).
 - ¹¹R. E. Grown, W. Grüebler, R. A. Hardekopf, F. D. Korrell, N. Jarmie, and G. G. Ohlsen, LASL Internal Report No. LA-7378-MS, 1978.
 - ¹²G. G. Ohlsen, G. C. Salzman, C. K. Mitchell, W. G. Simon, and W. Grüebler, Phys. Rev. C 8, 1639 (1973).
 - ¹³H. R. Bürgi, W. Grüebler, R. Hardekopf, G. Heidenreich, B. Jenny, V. König, J. Nurzynski, W. Reichart, R. Risler, H. Roser, P. A. Schmelzbach, and F. Seiler, SIN annual report, 1976, p. E90.
 - ¹⁴L. C. McIntyre and W. Haerberli, Nucl. Phys. A91, 382 (1967).
 - ¹⁵P. Darriulat, D. Garreta, A. Tarrats, and J. Arvieux, Nucl. Phys. A94, 653 (1967).
 - ¹⁶P. A. Schmelzbach, W. Grüebler, V. König, and P. Marmier, Helv. Phys. Acta 42, 573 (1969); P. A. Schmelzbach, W. Grüebler, V. König, and P. Marmier, Nucl. Phys. A184, 193 (1972).
 - ¹⁷W. Grüebler, P. A. Schmelzbach, V. König, R. Risler, and D. Boerma, Nucl. Phys. A242, 265 (1975).
 - ¹⁸H. H. Hackenbroich, P. Heiss, and Le-chi-niem, Nucl. Phys. A221, 461 (1974); B. Charnomordic, C. Fayard, and G. H. Lamot, Phys. Rev. C 15, 864 (1977).
 - ¹⁹S. E. Darden, R. M. Prior, and K. W. Corrigan, Phys. Rev. Lett. 25, 1673 (1970).
 - ²⁰V. König, W. Grüebler, A. Ruh, and R. E. White, P. A. Schmelzbach, R. Risler, and P. Marmier, Nucl. Phys. A166, 393 (1972).
 - ²¹W. Grüebler, P. A. Schmelzbach, V. König, R. Risler, B. Jenny, and D. Boerma, Nucl. Phys. A242, 285 (1975).
 - ²²H. E. Conzett, W. Dahme, Ch. Leemann, J. A. MacDonald, and J. P. Meulders (unpublished); see also H. E. Conzett, W. Dahme, Ch. Leemann, J. A. MacDonald and J. P. Meulders, in *Proceedings of the Fourth International Symposium on Polarization Phenomena in Nuclear Reactions*, edited by W. Grüebler and V. König (Birkhäuser, Basel, 1976), p. 566.
 - ²³D. J. Clark, A. U. Lucchio, F. Resmini, and H. Meiner, in *Proceedings of the Fifth International Cyclotron Conference* (Butterworths, London, 1971), p. 610.
 - ²⁴W. Haerberli, Annu. Rev. Nucl. Sci. 17, 373 (1967).
 - ²⁵*Proceedings of the Third International Symposium on Polarization Phenomena in Nuclear Reactions, Madison, Wisconsin, 1970*, edited by H. H. Barschall and W. Haerberli (University of Wisconsin, Madison, 1971), p. xxv.
 - ²⁶G. G. Ohlsen and P. W. Keaton, Jr., Nucl. Instrum. Methods 109, 41 (1973).
 - ²⁷G. G. Ohlsen, J. L. McKibben, G. P. Lawrence, P. W. Keaton, Jr., and D. D. Armstrong, Phys. Rev. Lett. 27, 599 (1971).
 - ²⁸R. E. Hintz, F. B. Selph, W. S. Flood, B. G. Harvey, F. G. Resmini, and E. A. McClatchie, Nucl. Instrum. Methods 72, 61 (1969); and extended in A. D. Bacher, E. A. McClatchie, M. S. Zisman, T. A. Weaver, and T. A. Tombrello, Nucl. Phys. A181, 453 (1972).
 - ²⁹J. T. C. Kan, Rev. Sci. Instrum. 44, 323 (1973).
 - ³⁰F. S. Goulding, D. A. Landis, J. Cerny, and R. H. Pehl, Nucl. Instrum. Methods 31, 1 (1964).
 - ³¹J. F. Janni, technical Report No. AFWL-TR-65-150, available from National Technical Information Service, Springfield, Va. 22151.
 - ³²F. Hinterberger, G. Mairle, U. Schmidt-Rohr, G. J. Wagner, and P. Turek, Nucl. Phys. A111, 265 (1968).
 - ³³H. Willmes, C. R. Messick, T. A. Cahill, D. J. Shadoan, and R. G. Hammond, Phys. Rev. C 10, 1762 (1974).
 - ³⁴H. J. Erramuspe and R. J. Slobodrian, Nucl. Phys. 49, 65 (1963).
 - ³⁵W. T. H. van Oers and K. W. Brockman, Jr., Nucl. Phys. 44, 546 (1963).
 - ³⁶H. W. Brock and J. L. Yntema, Phys. Rev. 135, B678 (1964).
 - ³⁷H. E. Conzett, F. Seiler, F. N. Rad, R. Roy, and R. M. Larimer, in *Proceedings of the Fourth International Symposium on Polarization Phenomena in Nuclear Reactions*, edited by W. Grüebler and V. König (Birkhäuser, Basel, 1976), p. 568.
 - ³⁸F. Seiler, F. N. Rad, H. E. Conzett, and R. Roy, Nucl. Phys. A296, 205 (1978).
 - ³⁹G. Heidenreich, J. Birchall, V. König, W. Grüebler, P. A. Schmelzbach, R. Risler, B. Jenny, and W. G. Weitkamp, in *Proceedings of the Fourth International Symposium on Polarization Phenomena in Nuclear Reactions*, edited by W. Grüebler and V. König (Birkhäuser, Basel, 1976), p. 570.